Dihadron, -hadron and +jet correlations in relativistic heavy-ion collisions

Guo-Liang Ma

Citation: AIP Conference Proceedings **1533**, 51 (2013); doi: 10.1063/1.4806776
View online: http://dx.doi.org/10.1063/1.4806776
View Table of Contents: http://scitation.aip.org/content/aip/proceeding/aipcp/1533?ver=pdfcov
Published by the AIP Publishing

Dihadron, γ-hadron and γ+jet correlations in relativistic heavy-ion collisions

Guo-Liang Ma

Shanghai Institute of Applied Physics, Chinese Academy of Sciences, P.O. Box 800-204, Shanghai 201800, China

Abstract. Within a multi-phase transport (AMPT) model, dihadron, γ-hadron and γ+jet azimuthal correlations are systematically studied. Because the large initial fluctuations generate all orders of harmonic flows, it is key step to remove flow background for dihadron correlation. However, it is not necessary for γ-hadron correlation since prompt photon does not flow. Dihadron and γ-hadron correlations are compared in Au+Au collisions at RHIC energy. In addition, the transverse momentum imbalance between prompt photon and jet is investigated in Pb+Pb collisions at LHC energy. Due to the strong interactions between jet and partonic matter, jet losses more energy in more central collisions which leads to a more larger imbalance. These three observables serve as complementary probes to learn more information about the interactions between jet and the formed matter at RHIC and LHC.

Keywords: jet, direct photon, correlation, RHIC, LHC
PACS: 25.75.-q, 25.75.Gz,25.75.Nq

INTRODUCTION

A strongly-coupling partonic matter has been created in relativistic heavy-ion collisions at RHIC and LHC [1]. Collective flow is a very sensitive tool for understanding bulk properties of the formed matter. It was predicted that the large pressure gradient transfers initial coordinate asymmetry into final momentum anisotropy via hydrodynamical evolution [2]. The RHIC experiment has measured anisotropic flow by extracting even orders of Fourier harmonic coefficients from the particle azimuthal distribution in momentum space with respect to the reaction plane [3]. It was recently found that event-by-event fluctuation of initial condition could induce odd orders of harmonic flows as well [4]. Therefore, the flow family of flow has been enlarged which includes all orders of anisotropies. On the other hand, jet is thought to be an important probe in experiment. Jet can losses energy and momentum by radiating gluons when it pass through the formed dense partonic medium, i.e. so-called jet quenching [5]. The lost energy must be redistributed into medium, which could lead to collective medium excitation. For example, Mach cone shock wave could be induced by a propagating jet inside medium [6, 7]. To study the medium excitation by jet, the azimuthal hadron correlation with respect to a leading high transverse momentum hadron, i.e. dihadron azimuthal correlation, is investigated experimentally [8, 9]. However, since two hadron are correlated due to the existence of flow background, it is necessary to remove the flow background to get jet-related signal. Since flow has all orders of components, it is important for dihadron study to well reconstruct the complete flow background.

To avoid the contamination of the flow background to jet-like correlation, a γ-jet is

8th China-Japan Joint Nuclear Physics Symposium
AIP Conf. Proc. 1533, 51-58 (2013); doi: 10.1063/1.4806776

TABLE 1. Two sets of the parameters a and b for the Lund string fragmentation and the QCD coupling constant α_s and the screening mass μ for the parton cross section σ in Au+Au 200GeV and in Pb+Pb (p+p) 2.76 TeV collisions in the AMPT simulations.

	a	**b**	α_s	μ	σ **(mb)**
Au+Au 200 GeV	2.2	0.5	0.47	1.8	10.0
Pb+Pb (p+p) 2.76 TeV	0.5	0.9	0.33	3.2	1.5

perfect tool for it. A γ-jet, including a direct (prompt) high-energy photon(γ) and a quark/gluon jet, is produced by hard processes of binary N+N collisions within the A+A overlapped area. Because γ does not interact with the medium strongly, it escapes the medium retaining the initial isotropic distribution, i.e. $v_n^\gamma = 0$. So the flow background is a constant for γ-hadron correlation. A comparative study between γ-hadron and di-hadron correlations can help us to approach a more complete picture about jet-medium interactions [10, 11]. Recent LHC experimental results based on full jet reconstruction disclose more detailed characterization of jet-medium interactions [12, 13]. The γ+jet measurements from CMS and ALTAS have provided the direct and less biased quantitative measure of jet energy loss in the medium, which present a deceasing jet-to-photon momentum imbalance ratio ($x_{j\gamma}$) from peripheral to central centrality bin in Pb+Pb collisions at $\sqrt{s_{\rm NN}}$ = 2.76 TeV [14, 15]. Afterwards, some theoretical efforts have been made to understand it [16, 17].

In this work, the AMPT model with string melting mechanism is chosen to study both hadron- and γ-triggered azimuthal correlations in most central Au+Au collisions (b = 0 fm) at $\sqrt{s_{NN}}$ = 200 GeV, with considering of the background subtraction including all orders of harmonic flows. In addition, an analysis about the imbalance of photon+jet are performed in Pb+Pb collisions at $\sqrt{s_{\rm NN}}$ = 2.76 TeV. All these studies give us more valuable insights into the interactions between jets and the formed medium in high energy heavy-ion collisions.

MODEL INTRODUCTION

The AMPT model with string meting scenario [18], which has shown good descriptions to many experimental observables [18, 19, 20, 21], is implemented in this work. The AMPT model includes four main stages of high energy heavy-ion collisions: the initial condition, partonic interactions, hadronization, and hadronic rescatterings. The initial condition, which includes the spatial and momentum distributions of minijet partons and soft string excitations, is obtained from HIJING model [22, 23]. For γ-hadron and γ-jet studies, three prompt photon production processes are included in the initial condition, including $q+\bar{q} \to g+\gamma$, $q+\bar{q} \to \gamma+\gamma$ and $q+g \to q+\gamma$ [24]. In the following, it starts the parton evolution with a quark and anti-quark plasma from the melting of strings. The parton cascade process, simulated by ZPC model [25], includes only elastic parton collisions at present whose cross sections (σ) are controlled by the values of strong coupling constant (α_s) and the Debye screening mass (μ). It recombines partons via a

simple coalescence model to produce hadrons when the partons freeze out. Dynamics of the subsequent hadronic matter is then described by ART model [26]. In this work, two AMPT model versions with different parameter sets are used to simulate Au+Au collisions at $\sqrt{s_{\rm NN}}$ = 200 GeV (σ=10 mb) [18], p+p and Pb+Pb collisions at $\sqrt{s_{\rm NN}}$ = 2.76 TeV (σ=1.5 mb) [27]. Table 1 lists the two sets of parameters for the simulations. For the simulations at LHC, a zero partonic interaction cross sections is also applied to simulate the physical scenario for hadronic rescatterings only, in order to compare with the other scenario with both parton cascade (1.5 mb) and hadronic rescatterings.

RESULTS AND DISCUSSIONS

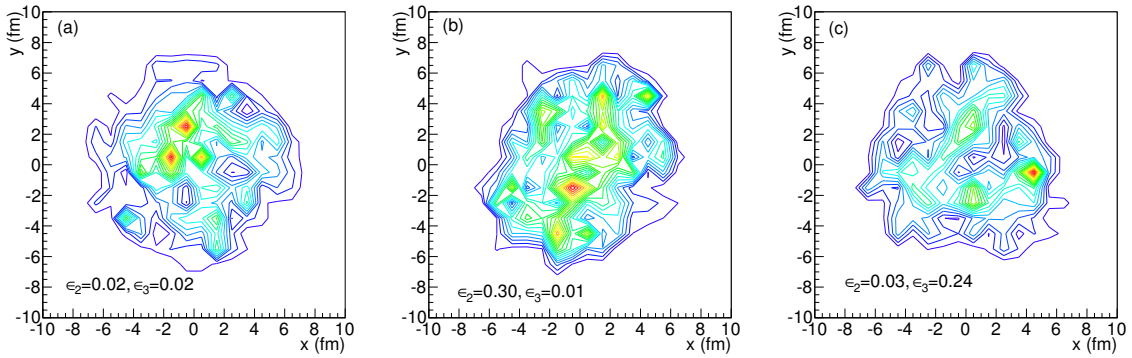

FIGURE 1. (Color online) Contour plots of initial parton density (in arbitrary units), $dN/dxdy$ in $x-y$ plane within a slice $|y| < 1$ fm for three typical AMPT events (Au+Au 200 GeV, b=0 fm).

Since a relativistic heavy-ion collision is dynamical evolution, it actually involves many important evolution stages. The initial state, as the beginning of the whole evolution, plays a very important role for final observables. In tradition, theorists treated it as a smooth energy or particle distribution. However, the initial state fluctuates event-by-event-ly, since energy is distributed around where each of hard nucleon pairs collide. Because these collisions randomly happen according to quantum fluctuations, it results in the fact that the initial state is not a smooth condition. Figure 1 (a)-(c) show initial parton density distributions ($dN/dxdy$) in $x-y$ plane within a slice $|y| < 1$ fm for three typical most central Au+Au AMPT events (b=0 fm). Due to large initial fluctuations, the initial geometry distribution is not isotropic any more even for b=0 fm events. It can appear in all kinds of different geometry shapes, such as Figure 1 (a) circle, (b) ellipse, and (c) triangle.

Similarly as the formation of elliptic flow, these initial geometry asymmetries can be translated to final momentum space by final interactions. Therefore all orders of anisotropies (harmonic flows) are formed finally. The left panel of Figure 2 displays the harmonic flows, v_n (n=1-6), of final hadrons for b=0 fm in Au+Au collisions at $\sqrt{s_{NN}} = 200$ GeV. It is obvious that the different orders of harmonic flows are not zero even for b=0 fm events.

These harmonic flows is so important that jet-like dihadon correlation will lose its importance without considering of them [4]. Since both hadrons have their flows in

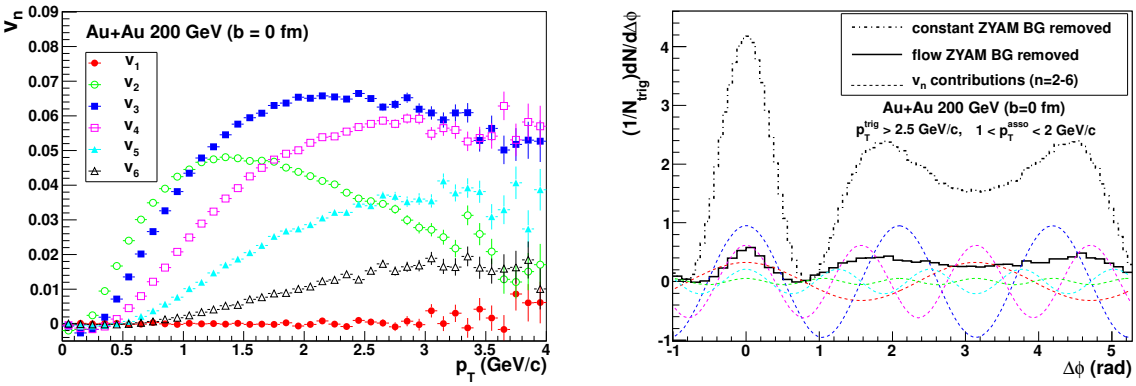

FIGURE 2. (Color online) Left panel: Azimuthal anisotropies of hadron spectra $v_n(p_T)$ $(n = 1-6)$ from AMPT calculations. Right panel: AMPT results on dihadron correlations before (dot-dashed) and after (solid) subtraction of the contribution from harmonic flows v_n (n=2-6) (dashed). Both panel ares for Au+Au collisions at $\sqrt{s_{\rm NN}}$ = 200 GeV (b = 0 fm, 10mb).

dihadron correlation, it is a critical point for the dihadron study how to completely remove harmonic flow background to see the medium excitation by jet. The right panel of Figure 2 shows dihadron correlations before (dot-dashed) and after (solid) the removal of contributions from harmonic flows for $p_T^{\rm trig} > 2.5$ GeV/c and $1 < p_T^{\rm asso} < 2$ GeV/c. The contributions from each harmonic flow, $n = 2$-6 (dashed), are also shown. These contributions are significant up to $n = 5$ harmonics. The remained signal is quite small in comparison with the subtracted background. Therefore, it becomes a key question for the experimental research on dihadron correlation how to control the harmonic flow background originated from initial fluctuations.

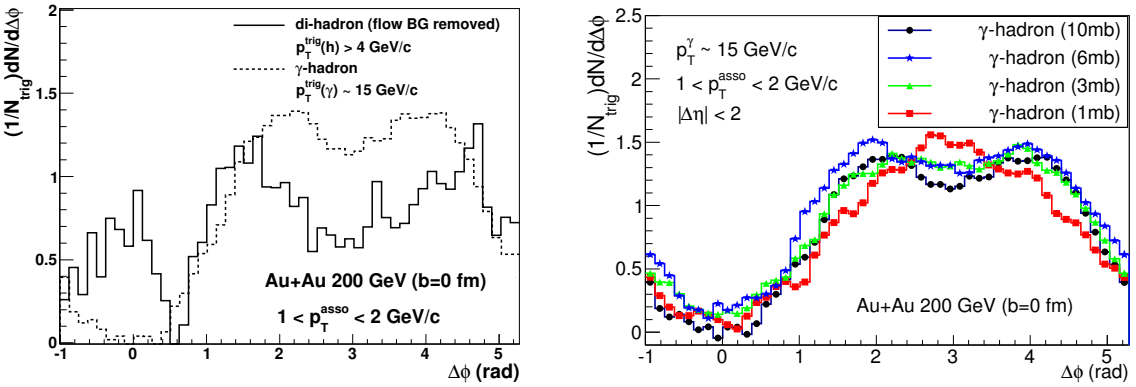

FIGURE 3. (Color online) Left panel: Dihadron correlation (solid) compared with γ-hadron correlation (dashed) in Au+Au collisions (10 mb). Right panel: γ-hadron correlations with different values of parton cross section. Both panel ares for Au+Au collisions at $\sqrt{s_{\rm NN}}$ = 200 GeV (b = 0 fm) from AMPT model calculations.

On the other hand, γ-hadron azimuthal correlation has a good advantage over di-hadron, because direct (prompt) photons only attend electromagnetic interactions with

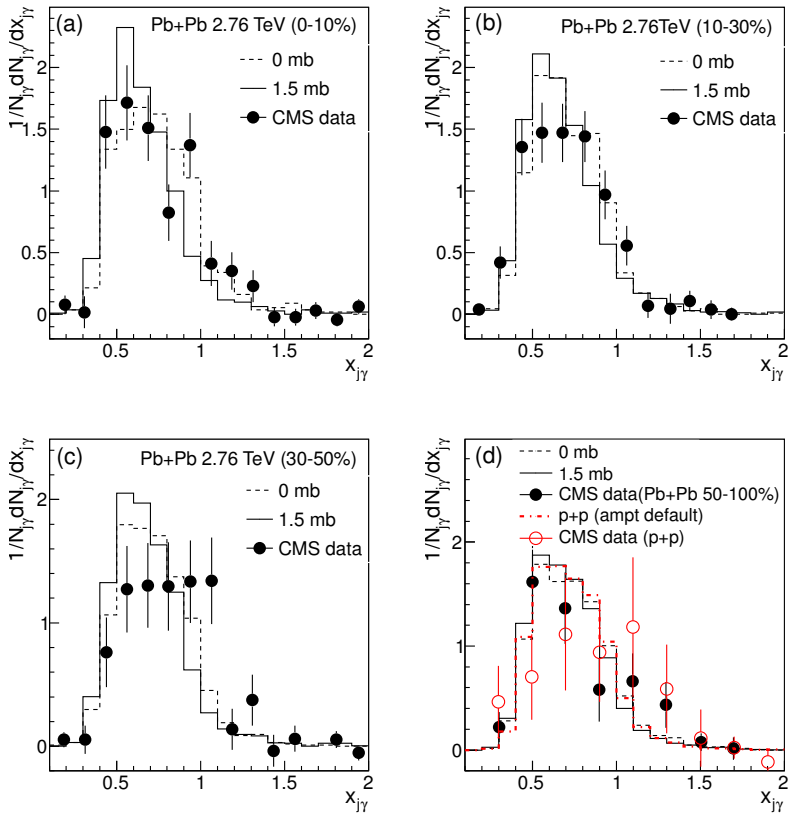

FIGURE 4. The distributions of imbalance ratio $x_{j\gamma}$=p_T^{jet}/p_T^{γ} between the photon ($p_T^{\gamma} > 60$ GeV/c) and jet ($p_T^{jet} > 30$ GeV/c, $\Delta\phi_{j\gamma} > 7\pi/8$) after background subtraction for four centrality bins in Pb+Pb and p+p collisions, where the solid and dash (dot-dash) histograms represent the AMPT results with a 1.5 mb or 0 mb parton cross section respectively, while the circles represent the data from CMS experiment [14].

medium and do not flows. Therefore, there is no flow background issue for γ-hadron correlation. The left panel of Figure 3 shows that γ-hadron correlation ($p_T^{\rm trig}(\gamma) \sim 15$ GeV/c and $1 < p_T^{\rm asso} < 2$ GeV/c) is comparable with dihadron correlation in magnitude but with a less pronounced double-peak, which can be attributed to additional dihadron correlations from hot spots, geometric bias toward surface, and tangential emissions that enhance deflections of jet showers and jet-induced medium excitations by radial flow [10]. Shown in the right panel of Figure 3 are γ-hadron correlations in central Au+Au collisions at $\sqrt{s_{\rm NN}}$ = 200 GeV with different values of parton cross section. The away-side structure changes from single peak to double peaks and the splitting of double peaks increases, with the increasing of parton cross section. It is consistent with the scenario that jet losses its energy to excite the partonic medium in a Mach-like cone mode [11].

Recently, the photon+jet measurements from CMS and ALTAS have provided the direct and less biased quantitative measure of jet energy loss in the medium, which present a deceasing jet-to-photon momentum imbalance ratio ($x_{j\gamma}$) from peripheral to central centrality bin in Pb+Pb collisions at $\sqrt{s_{\rm NN}}$ = 2.76 TeV [14, 15]. It is interesting

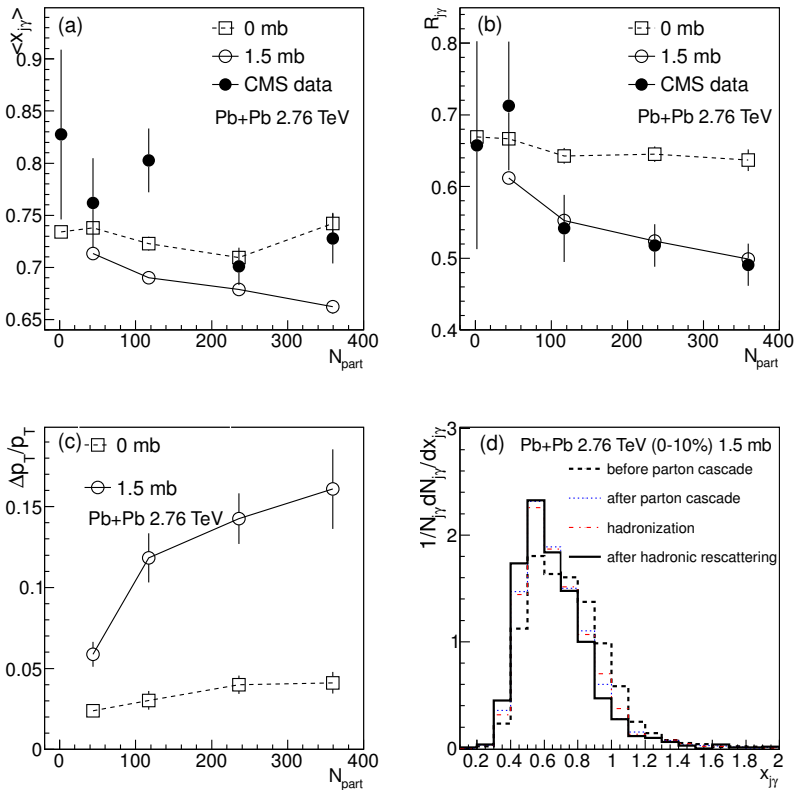

FIGURE 5. (a) Average ratio $\langle x_{j\gamma} \rangle$ as functions of N_{part}. (b) Average ratio of photon with an associated jet above 30 GeV/c as functions of N_{part}. (c) Average energy loss fraction of jet $\langle \Delta p_T / p_T \rangle$ as functions of N_{part}. (d) The distributions of imbalance ratio $x_{j\gamma}$ at different evolution stages in most central Pb+Pb events (0-10%).

to explore the jet energy loss features by using the full reconstructed jet technique. In these LHC measurements, the transverse momentum imbalance is defined as the ratio of $x_{j\gamma}$=p_T^{jet}/p_T^{γ} to study jet energy loss mechanism experimentally. The anti-k_t algorithm from the standard fastjet package is made use of to reconstruct the full jet [28]. Jet cone size is set to be 0.3 (R=0.3) , p_T of jet is larger than 30 GeV/c ($p_T^{jet} > 30$ GeV/c) and pseudorapidity of jet is within a mid-rapidity gap of 1.6 ($|\eta^{jet}| < 1.6$). The jet background is locally estimated within a pseudorapidity strip $\Delta\eta < 1.0$ and removed in jet reconstruction. Both jet energy scale and jet efficiency corrections, which are obtained by combining triggered p+p and non-triggered Pb+Pb events, have been applied for each jet. The triggered photons are weighted with the experimental measured prompt photon p_T spectra finally. Figure 4 (a)-(d) show the simulation results on the imbalance ratio distributions for four centrality bins in Pb+Pb collisions and p+p collisions at $\sqrt{s_{\rm NN}}$ = 2.76 TeV.

To learn why and how the imbalances are produced, the corresponding averaged values of imbalance ratio $\langle x_{j\gamma} \rangle$ as functions of number of participant nucleons (N_{part}) are presented in Figure 5 (a). The AMPT results with both partonic interactions and

hadronic rescatterings (i.e. 1.5 mb) give the smaller $x_{j\gamma}$ and $\langle x_{j\gamma} \rangle$ than those with hadronic rescatterings only (i.e. 0 mb) and experimental data. It indicates that the strong interactions between jet and partonic matter can result in larger momentum asymmetry than those between jet and hadronic matter, meanwhile which is more stronger in more central collisions. On the other hand, Figure 5 (b) shows that though the AMPT result with partonic interactions slightly underestimate the experimental observable of $R_{j\gamma}$, but it can well reproduce the fraction of photons that have an associated jet with $p_T^{jet} > 30$ GeV/c, which also supports the picture of jet quenching in partonic matter at LHC. To quantitively learn how much jet losses its energy in partonic or hadronic matter, the averaged energy loss fractions of jet, $\langle \Delta p_T / p_T \rangle = \left\langle (p_T^{jet,initial} - p_T^{jet,final}) / p_T^{jet,initial} \right\rangle$, are shown for the four centrality bins in Figure 5 (c). Jet losses its energy from by $\sim$15% in central collisions down to by $\sim$5% in peripheral collisions due to partonic interactions, however hadronic interactions only can give much smaller energy losses from $\sim$4% to $\sim$2%.

Because a heavy-ion collision actually is a dynamical evolution which involves many different stages, it is very essential to see the effect separately from other stages on the imbalance. Figure 5 (d) gives the distributions of imbalance ratio $x_{j\gamma}$ at different evolution stages for most central Pb+Pb collisions. It is found that jet mainly losses its energy during the stage of parton cascade, and the following hadronization and hadronic rescattering do not change the $x_{j\gamma}$ distribution much more. Therefore, photon+jet measurements do reflect the information about the interactions between jet and partonic matter.

CONCLUSIONS

Harmonic flows can arise from large initial fluctuations, so harmonic flow background significantly affects dihadron correlation. However γ-hadron correlation is proposed as a golden probe, because it can only be caused by jet-medium interactions. For the study of γ+jet, the transverse momentum imbalance between prompt γ and jet is produced by strong partonic interactions between jet and partonic medium. The final hadronic interactions have little effect on the final observed imbalance. The systematic studies about dihadron, γ-hadron and γ+jet correlations provide important integral parts of jet-medium interactions at RHIC and LHC.

ACKNOWLEDGMENTS

This work was supported by the NSFC of China under Projects Nos. 11175232, 11035009, the Knowledge Innovation Program of Chinese Academy of Sciences under Grant No. KJCX2-EW-N01, the Project-sponsored by SRF for ROCS, SEM, CCNU-QLPL Innovation Fund (QLPL2011P01).

REFERENCES

1. I. Arsene et al.[BRAHMS Collaboration], Nucl. Phys. A **757**, 1 (2005); B. B. Back et al. [PHOBOS Collaboration], Nucl. Phys. A **757**, 28 (2005); J. Adames et al. [STAR Collaboration], Nucl. Phys. A **757**, 102 (2005); S. S. Adler et al. [PHENIX Collaboration], Nucl. Phys. A **757**, 184 (2005).
2. P. F. Kolb and U. W. Heinz, In *Hwa, R.C. (ed.) et al.: Quark gluon plasma* 634-714 [nucl-th/0305084].
3. J. Adams *et al.* [STAR Collaboration], Phys. Rev. C **72**, 014904 (2005) [nucl-ex/0409033].
4. B. Alver and G. Roland, Phys. Rev. C **81**, 054905 (2010) [Erratum-ibid. C **82**, 039903 (2010)] [arXiv:1003.0194 [nucl-th]].
5. X. -N. Wang and M. Gyulassy, Phys. Rev. Lett. **68**, 1480 (1992).
6. J. Casalderrey-Solana, E. V. Shuryak and D. Teaney, J. Phys. Conf. Ser. **27**, 22 (2005) [Nucl. Phys. A **774**, 577 (2006)] [hep-ph/0411315].
7. H. Stoecker, Nucl. Phys. A **750**, 121 (2005) [nucl-th/0406018].
8. J. Adams *et al.* [STAR Collaboration], Phys. Rev. Lett. **95**, 152301 (2005) [nucl-ex/0501016].
9. S. S. Adler *et al.* [PHENIX Collaboration], Phys. Rev. Lett. **97**, 052301 (2006) [nucl-ex/0507004].
10. G. L. Ma and X. N. Wang, Phys. Rev. Lett. **106** ,162301 (2011) arXiv:1011.5249 [nucl-th].
11. H. Li, F. Liu, G. L. Ma, X. -N. Wang and Y. Zhu, Phys. Rev. Lett. **106**, 012301 (2011) [arXiv:1006.2893 [nucl-th]].
12. G. Aad *et al.* [Atlas Collaboration], Phys. Rev. Lett. **105**, 252303 (2010) [arXiv:1011.6182 [hep-ex]].
13. S. Chatrchyan *et al.* [CMS Collaboration], Phys. Rev. C **84**, 024906 (2011) [arXiv:1102.1957 [nucl-ex]].
14. S. Chatrchyan *et al.* [CMS Collaboration], arXiv:1205.0206 [nucl-ex].
15. [ATLAS Collaboration], ATLAS-CONF-2012-121.
16. W. Dai, I. Vitev and B. -W. Zhang, arXiv:1207.5177 [hep-ph].
17. G. Y. Qin, arXiv:1210.6610 [hep-ph].
18. Z. W. Lin, C. M. Ko, B. A. Li, B. Zhang and S. Pal, Phys. Rev. C **72**, 064901 (2005) [arXiv:nucl-th/0411110].
19. J. H. Chen, Y. G. Ma, G. L. Ma *et al.*, Phys. Rev. C **74**, 064902 (2006).
20. B. Zhang, L. W. Chen and C. M. Ko, Phys. Rev. C **72**, 024906 (2005) [arXiv:nucl-th/0502056].
21. G. L. Ma and B. Zhang, Phys. Lett. B **700**, 39 (2011) [arXiv:1101.1701 [nucl-th]].
22. X. N. Wang and M. Gyulassy, Phys. Rev. D **44**, 3501 (1991).
23. M. Gyulassy and X. N. Wang, Comput. Phys. Commun. **83**, 307 (1994) [arXiv:nucl-th/9502021].
24. T. Sjöstrand, Comput. Phys. Commun. **82**, 74 (1994).
25. B. Zhang, Comput. Phys. Commun. **109**, 193 (1998) [arXiv:nucl-th/9709009].
26. B. A. Li and C. M. Ko, Phys. Rev. C **52**, 2037 (1995) [arXiv:nucl-th/9505016].
27. J. Xu and C. M. Ko, Phys. Rev. C **83**, 034904 (2011) [arXiv:1101.2231 [nucl-th]].
28. M. Cacciari, G. P. Salam and G. Soyez, Eur. Phys. J. C **72**, 1896 (2012) [arXiv:1111.6097 [hep-ph]].